Measurement of ^{55}Fe(n,p) cross sections by the surrogate-reaction method for fusion technology applications

Bhawna Pandey, V. V. Desai, S. V. Suryanarayana, B. K. Nayak, A. Saxena, E. T. Mirgule, S. Santra, K. Mahata, R. Makawana, M. Abhangi, T. K. Basu, C. V. S. Rao, S. Jakhar, S. Vala, B. Sarkar, H. M. Agrawal, G. Kaur, P. M. Prajapati, Asim Pal, D. Sarkar, and A. Kundu

Phys. Rev. C **93**, 021602 — Published 18 February 2016

DOI: 10.1103/PhysRevC.93.021602

Measurement of ^{55}Fe(n,p) cross-sections by Surrogate Reaction Method for fusion technology applications

Bhawna Pandey [1*], V.V. Desai [2,†] S.V. Suryanarayana [2], B.K. Nayak [2,‡] A. Saxena [2], E.T. Mirgule [2], S. Santra [2], K. Mahata [2], R. Makawana [3], M. Abhangi [1], T.K. Basu [1], C.V.S. Rao [1], S. Jakhar [1], S. Vala [1], B. Sarkar [1], H.M. Agrawal [4], G. Kaur [5], P.M. Prajapati [3], Asim Pal [2], D. Sarkar [2], and A. Kundu [2]

[1] *Fusion Neutronics Laboratory, Institute for Plasma Research, Bhat, Gandhinagar 382428, India*

[2] *Nuclear Physics Division, Bhabha Atomic Research Centre, Mumbai 400085, India*

[3] *Physics Department, Faculty of Science, M.S. University of Baroda 390002, Vadodara, India*

[4] *Department of Physics, G.B. Pant University of Ag. and Tech. Pantnagar, Uttarakhand 263145, India*

[5] *Department of Physics, Panjab University, Chandigarh 160014, India*

The proton decay probabilities of ^{56}Fe* and ^{47}Ti* compound systems have been measured, which are populated by transfer reactions ^{52}Cr(^{6}Li,d)^{56}Fe* (surrogate of n+^{55}Fe $\rightarrow$ ^{56}Fe* $\rightarrow$ p+ ^{55}Mn) and ^{45}Sc(^{6}Li,α)^{47}Ti* (surrogate of n+ ^{46}Ti $\rightarrow$ ^{47}Ti* $\rightarrow$ p+^{46}Sc) reactions respectively. The ^{55}Fe(n,p) cross-sections are then obtained in the equivalent neutron energy range of 7.9 MeV to 20.1 MeV within the framework of surrogate ratio method. The measured results have been compared with predictions of EMPIRE - 3.2.3 statistical model code and various recent evaluated data libraries. The experimental cross-section data on ^{55}Fe(n,p) are in reasonable agreement with EAF-2010 while TENDL-2014 and ROSFOND-2010 show some discrepancies. Present study demonstrates the possibility of determining neutron induced charged particle emission cross-sections for unstable radio nuclide relevant for fusion technology applications by surrogate reaction method.

PACS numbers: 25.85.Ec 24.75.+i

Fusion of light nuclei has the potential to become one of the long term options for the supply of energy with a moderate impact on the environment. International efforts are presently being made in a coordinated and cooperative manner to build International Thermonuclear Experimental Reactor (ITER) based on the concept of magnetic confinement of plasma, for net fusion energy production [1]. Although different isotopes of light elements can be paired to achieve fusion, the deuterium - tritium (D-T) reaction has been identified as the most efficient for fusion devices. For the designing and building of current fusion reactor a number of materials - both structural and functional are required to be developed. The environmental and safety aspects of fusion reactors depend significantly on material choice [2]. As the materials have to face the high fluence of 14.1 MeV neutrons in the fusion reactor, the structural materials should have low activation, good thermo-mechanical properties and high radiation resistance. Finalizing the specifications for materials, their development, characterization, production and suitable fabrication into components is a major challenge. Moreover, these high energy neutrons cause (n,p) and (n,α) reactions with almost all elements, leading to the formation of both helium and hydrogen which can cause serious damage to the structural materials [3]. Therefore the cross-section data of the neutron induced reactions with the structural materials have a critical importance on fusion reactor design. Generally stainless steel (SS) is used as a structural material having Fe, Ni, Cr, Mn, Co, and Nb as main constituents (in SS316 content of Fe$\sim$65%). The neutron induced transmutation reactions with these elements in the initial SS composition leads to the formation of large numbers of radionuclide in the mass region $\sim$50–60 such as ^{53}Mn ($T_{1/2}$=3.74$\times$10^6 year),^{55}Fe($T_{1/2}$=2.73 year), ^{60}Fe ($T_{1/2}$=1.5$\times$10^6 year), ^{60}Co($T_{1/2}$=5.27 year), ^{59}Ni ($T_{1/2}$=7.6$\times$10^4 year), and ^{63}Ni ($T_{1/2}$ =100.1 year) inside the fusion reactor [4]. This may lead to significant long-term waste disposal and radiation damage issues [5–7]. Fusion neutronics studies have been done so far considering only the stable isotopes of Cr, Fe, and Ni. But in a D - T fusion reactor, large amount of radio nuclides will be produced during reactor operation as well as after shut-down, which may affect neutronics of the reactor [8].

The ^{55}Fe is a primary dominant radio-nuclide produced during the operation as well as after shut down of the fusion reactor by neutron induced reactions via ^{56}Fe(n,2n), ^{54}Fe(n,γ), ^{59}Co(n,α)^{56}Mn(β^-)^{56}Fe(n,2n), and ^{58}Ni(n,α) as shown by pathways in Fig.1. The exposure of natural iron material in the initial SS composition to high neutron flux will produce high amounts of ^{55}Fe via the threshold reaction ^{56}Fe(n,2n)^{55}Fe [4, 7]. The activation analysis carried out assuming $1.043\times10^{15} n/cm^2/s$ on first wall during 5 full power year (FPY) on 1 kg pure iron sample, shows that the ^{55}Fe activities are 4.07×10^{14} Bq/kg just after irradiation [9]. This corresponds to production of ^{55}Fe $\sim$ 4.5 gm/kg of pure iron. These nuclei will interact with slow and fast neutrons and produce large amount of hydrogen and helium which lead to the swelling and embrittlement of the first wall and

*Presently at Department of Physics, G.B. Pant University of Ag. and Tech. Pantnagar, Uttarakhand 263145, India

†Electronic address: vvdesai@barc.gov.in

‡Electronic address: bknayak@barc.gov.in

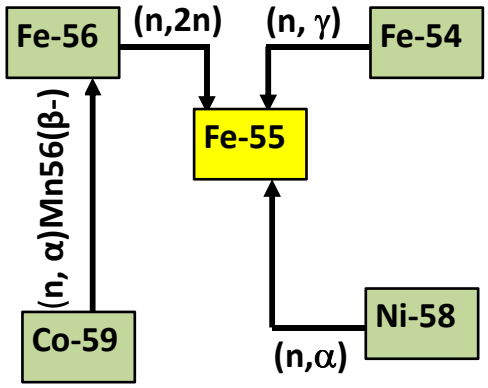

FIG. 1: Schematic of ^{55}Fe formation pathways in typical fusion reactor.

other structural materials. Therefore the neutron induced cross-sections of ^{55}Fe(n,p)^{55}Mn reaction are crucial for the fusion reactor from neutronics point of view [10, 11].

As of today, there is no direct experimental measurement of the ^{55}Fe (n,p) cross-section because of the unavailability of ^{55}Fe target in nature. When direct experimental determination of compound nuclear cross-sections is difficult, indirect methods are often used. The surrogate nuclear reaction technique is such an indirect method for determining the compound nuclear cross section for a particular type of 'desired' reaction, namely a two-step reaction, a + A $\rightarrow$ B* $\rightarrow$ c + C, that proceeds through a compound nuclear state B*. This method was first proposed by J.D. Cramer and H.C. Britt in the 1970s to estimate neutron-induced fission cross sections from transfer reactions [12, 13]. In a compound reaction, target and projectile nuclei combine to form a highly excited, intermediate system, the compound nucleus, which subsequently decays. The reaction proceeds on a relatively slow time scale ($\gg 10^{-22}$sec), as the formation of a compound nucleus involves the excitation of many degrees of freedom. Apart from observing the constraints of basic conservation laws (energy, angular momentum), the formation and decay of a compound nucleus are considered to be independent of each other in first order which is "Bohr hypothesis". This independence is exploited in the surrogate - reaction approach. Moreover, the surrogate reaction method also invokes the approximation that, the decay of the compound nucleus is independent of the angular momentum and parity of the populated state which is known as the Weisskopf - Ewing limit of Hauser - Feshbach theory or Weisskopf - Ewing approximation. In such situations, the cross section for the 'desired' reaction can be expressed as $\sigma_{\alpha\beta}(E_{ex}) = \sigma_{\alpha}^{CN}(E_{ex}) \times \Gamma_{\beta}(E_{ex})$ [17, 18]. Here α denotes the entrance channel (a + A) and β represents the relevant exit channel (c + C). The formation cross section $\sigma_{\alpha}^{CN}(E_{ex}) = \sigma(a + A \rightarrow B^*)$ can be calculated to a reasonable accuracy by using optical potentials, while the theoretical decay probabilities $\Gamma_{\beta}(E_{ex})$ for the different decay channels β are often quite uncertain. The objective of the Surrogate method is to obtain these decay probabilities experimentally. The desired reaction a + A $\rightarrow$ B* $\rightarrow$ c + C which leads to the compound system B* at an excitation energy (E_{ex}) can decay through different exit channels: fission, gamma-decay, neutron and charged particle emission. In a Surrogate experiment, the compound nucleus B* occurring in the desired reaction(a + A $\rightarrow$ B* $\rightarrow$ c + C) that involves unstable targets is produced via an alternate (surrogate) direct reaction (d + D $\rightarrow$ b + B*) which involves a stable projectile-target combination (d + D). The transfer reaction (d + D $\rightarrow$ b + B*) leads to the formation of compound system B* and ejectile b. The identification of the ejectile permits to determine the mass (A) and charge (Z) of the decaying nucleus. In addition, the excitation energy (E_{ex}) of the nucleus A is determined by employing the two-body kinematics. Also the measurement of the number of coincidences between the ejectiles (b) and the decay channel (β) normalized to the total number of detected ejectiles allows one to extract the decay probability $\Gamma_{\beta}(E_{ex}) = \frac{N_{\beta-b}}{N_b}$ for the corresponding decay channel. Within the framework of surrogate reaction method, the cross section $\sigma_{\alpha\beta}(E_{ex})$ for the corresponding decay channel β for the desired reaction is then deduced from the product of the decay probability measured in the surrogate reaction and the compound nucleus formation cross section for the desired reaction [12]. The compound nucleus formation cross-section for desired reaction is obtained from optical model calculations. The compound nucleus excitation energy can be translated into equivalent neutron energy E_n via the relation $E_n = \frac{A+1}{A}(E_{ex} - S_n)$, where S_n is the neutron separation energy of the compound nucleus [14]. In a transfer reaction residual compound system is populated over a wide range of excitation energy. Therefore, with fixed beam energy, the surrogate method allows to determine the cross sections over a wide range of equivalent neutron energy.

In recent years, surrogate reaction method has been extensively used to determine neutron induced fission cross sections for a large number of actinide targets [14–16]. Some efforts were also made to determine neutron capture cross-sections [17, 18]. But so far no attempts have been made to determine compound nuclear particle emission cross-sections using surrogate reaction method. In the present work, the ^{55}Fe(n,p) reaction cross-sections have been obtained from measurements of the ratio of proton decay probabilities of ^{56}Fe* and ^{47}Ti* compound nuclei over the excitation energy range 19 - 30 MeV. The ^{56}Fe* and ^{47}Ti* compound nuclei at similar excitation energies are produced in ^{52}Cr(^{6}Li,d)^{56}Fe* and ^{45}Sc(^{6}Li,α)^{47}Ti* transfer reactions at $E_{\rm lab}$=33.0 MeV and 35.75 MeV respectively. The reaction n+ ^{46}Ti $\rightarrow$ ^{47}Ti* $\rightarrow$ p+^{46}Sc cross-sections value as function of excitation energy has been used as the reference to determine the n+^{56}Fe $\rightarrow$ ^{56}Fe* $\rightarrow$ p+ ^{55}Mn cross-section from the measured ratio of the decay probabilities of ^{56}Fe* and ^{47}Ti* compound systems.

The experiment was performed at Bhabha Atomic Research Centre - Tata Institute of Fundamental Research (BARC-TIFR) 14-MV Pelletron accelerator facility at Mumbai. The self-supporting thin metallic targets of ^{nat}Cr (abundance ^{52}Cr $\sim$ 84%) and ^{45}Sc (abundance = 100%) of thickness 500 μg/cm^2 prepared by thermal evaporation technique were bombarded with ^{6}Li beam at incident energies $E_{\rm lab}$= 33.0 MeV and 35.75 MeV respectively. The transfer reactions, relevant ground state Q-values ($Q_{\rm gg}$), compound nucleus, neutron separation energies and corresponding surrogate neutron-induced reactions are listed in Table I. The two silicon surface barrier (SSB) ΔE-E detector telescopes with ΔE detector of thickness 150μm and 100 μm and identical E detector of thickness of 1 mm were mounted at angles of 25° and 35° with respect to beam direction around the transfer grazing angle to identify the projectile-like fragments (PLFs).

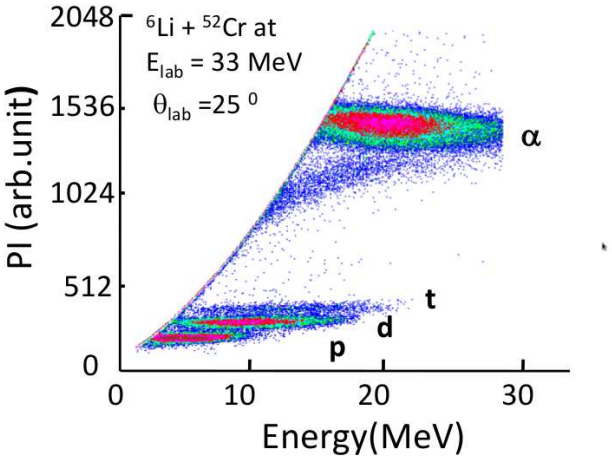

FIG. 2: Particle Identification (PI) vs total energy ($E_{\rm tot}$) plot of PLF produced in ^{6}Li+ ^{52}Cr reaction at $E_{\rm lab}$=33.0 MeV.

TABLE I: Transfer reactions investigated in present experiment, their ground state Q-values (Q_{gg}) and corresponding surrogate neutron - induced reactions.

Transfer reaction reaction	Q_{gg} (MeV)	CN	S_n (MeV)	Neutron-induced reaction
^{52}Cr(^{6}Li,d)	6.139	^{56}Fe	11.197	^{55}Fe(n,p)
^{45}Sc(^{6}Li,α)	15.527	^{47}Ti	13.189	^{46}Ti(n,p)

The proton, deuteron, triton and alpha are uniquely identified by plotting ΔE against the residual energy ($E_{\rm res}$) in the E detector. This plot was then converted to

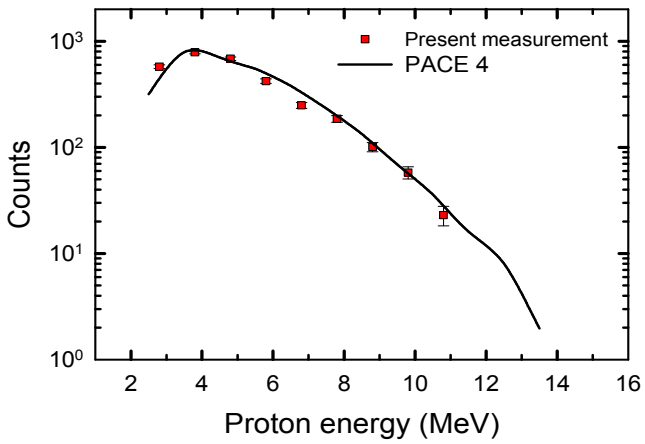

FIG. 3: Measured proton proton energy spectra in coincidence with deuteron PLF at $\theta_{\rm lab}$ = 130° for ^{6}Li+ ^{52}Cr reaction at 33.0 MeV. Also the prediction of PACE4 statistical model is shown as continuous line.

effective particle identification (PI) versus total energy plot. This has been generated using the linearization function (PI= b×($E_{\rm tot}^{1.70}$ – $E_{\rm res}^{1.70}$)), where $E_{\rm tot}$ is the total particle energy, $E_{\rm res}$ is the energy deposited in the E detector, and b is a constant. The Fig.2 shows a typical PI versus total energy plot, where all PLF's are clearly identified. The compound nuclei ^{56}Fe and ^{47}Ti formed in ^{52}Cr(^{6}Li,d)^{56}Fe* and ^{45}Sc(^{6}Li,α)^{47}Ti* transfer reactions are identified by outgoing d and α PLFs, respectively. A large area 16 strip solid state detector (each strip of size 3.1 mm×50.0 mm, ΔE=60 μm and E=1500μm) was placed at a back angle 130° with respect to beam direction with an angular opening of 16° to detect the decay proton in coincidence with PLFs. The typical outgoing evaporated proton spectra from compound system ^{56}Fe* in coincidence with PLF (deuteron) is shown in Fig.3, along with the predictions of statistical model code PACE4 [19]. It can be seen that PACE4 predictions compare well with the experimental proton spectrum confirming the evaporation nature of the proton emission. The time correlation between PLFs and decay particles (proton) are recorded through a time to amplitude converter (TAC). A typical TAC versus PLF deuteron energy plot in ^{6}Li+^{52}Cr reaction at $E_{\rm lab}$=33.0 MeV is shown in Fig.4.

The ground state ($Q_{\rm gg}$) for ^{52}Cr(^{6}Li,d)^{56}Fe* and ^{45}Sc(^{6}Li,α)^{47}Ti* transfer reactions are 6.139 MeV and 15.527 MeV respectively. The ^{56}Fe* and ^{47}Ti* compound systems are populated at overlapping excitation energies in the range of 19-30 MeV in ^{6}Li+^{52}Cr→ d+ ^{56}Fe* transfer reaction ($E_{\rm lab}$(^{6}Li)=33.0 MeV) and ^{6}Li+^{45}Sc → α+ ^{47}Ti* transfer reaction ($E_{\rm lab}$(^{6}Li)=35.75 MeV) respectively. The proton decay probabilities of ^{56}Fe* and ^{47}Ti* compound nuclei produced in the transfer reactions are obtained from Eq.1.

$$\Gamma_p^{CN}(E_{\rm ex}) = \frac{N_{i-p}(E_{\rm ex})}{N_i(E_{\rm ex})}, \qquad (1)$$

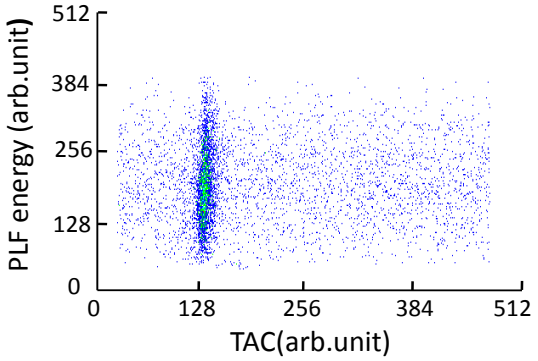

FIG. 4: Typical PLF-proton TAC versus PLF deuteron energy plot in ^{6}Li+ ^{52}Cr reaction at $E_{\rm lab}$=33.0 MeV.

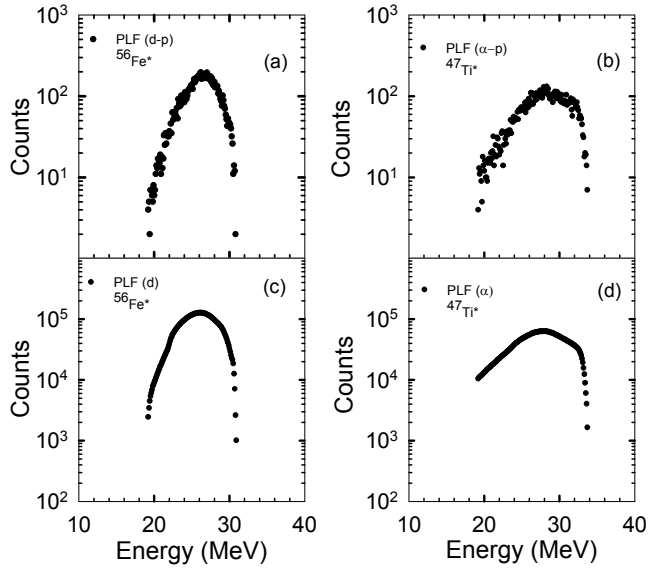

FIG. 5: Excitation energy spectra of the target like fragments produced in ^{6}Li+ ^{52}Cr and ^{6}Li+ ^{45}Sc reactions corresponding to PLF deuteron and alpha with ((a), (b)) and without ((c), (d)) coincidence with evaporated proton.

where, i denotes the deuteron or alpha PLF channels corresponding to the ^{56}Fe* or ^{47}Ti* compound nucleus. N_i and N_{i-p} denotes the singles and coincidence counts respectively, at excitation energy $E_{\rm ex}$

The telescopes and strip detector were energy calibrated by using the ^{229}Th source and in an in beam experiment that made use of ^{16}O* excited states formed in the ^{12}C(^{6}Li, d)^{16}O* reaction at 18 MeV. The excitation energy spectra of target like residues of ^{56}Fe* and ^{47}Ti* were determined by employing two body kinematics for deuteron and alpha PLF channels. The excitation energy spectra so obtained for ^{56}Fe* and ^{47}Ti* nuclei are shown in Fig.5. The excitation energy spectra obtained for PLF-proton coincidence are also shown in the same figure. The ratio of coincidence to single counts were determined in steps of 1.0 MeV excitation energy bin in the energy range 19-30 MeV for ^{56}Fe* and ^{47}Ti* compound systems. The relative proton decay probabilities for same excitation energy bin are multiplied with the relative neutron-induced compound nuclear formation cross-sections to obtain the ratio of the compound nuclear reaction cross-sections as follows:

$$\frac{\sigma^{^{55}Fe(n,p)}(E_{ex})}{\sigma^{^{46}Ti(n,p)}(E_{ex})} = R(E_{ex}) = \frac{\sigma_{CN}^{n+^{55}Fe}(E_{ex})}{\sigma_{CN}^{n+^{46}Ti}(E_{ex})}\frac{\Gamma_{p}^{^{56}Fe}(E_{ex})}{\Gamma_{p}^{^{47}Ti}(E_{ex})}. \quad (2)$$

The ^{46}Ti(n,p) reaction cross-section is used as the reference monitor and taken from IRDFF-1.05 (International Reactor Dosimetry Fusion File) [20]. The neutron capture cross-section were calculated by EMPIRE-3.2.3 code for ^{56}Fe* and ^{47}Ti* compound systems in the excitation energy range 19 to 30 MeV. Using Eq.2 the ^{55}Fe(n,p) cross-section as a function of excitation energy of ^{56}Fe* were obtained over the excitation energy range 19-30 MeV. The excitation energy was converted to equivalent neutron energy in the range of 7.9 MeV to 20.1 MeV by subtracting the neutron separation energy of ^{56}Fe (Sn= 11.197 MeV). The present experimental result of ^{55}Fe(n,p) cross-sections as a function of equivalent neutron kinetic energy are shown in Fig.6.

Statistical model calculations have been carried out using EMPIRE-3.2.3 code [21] to understand quantitatively the ^{55}Fe(n,p) reaction cross sections in the neutron energy range 1.0 MeV to 20.0 MeV. The standard Hauser Feshbach formalism [22] was applied to calculate the compound nuclear decay [23]. The input parameters in the calculations such as nuclear masses, ground state deformations, discrete energy levels and decay schemes, nuclear level densities, moment of inertia, and gamma ray strength functions are taken from "Reference Input Parameter Library" RIPL-3 [24]. We have used global optical model parameters for both neutrons and protons by Koning and Delaroche [25]. The level density was calculated using the dynamic approach specific to the EMPIRE code based on Enhanced Generalized Superfluid Model with Mayers-Swiatecki shell corrections, including collective enhancements of the level densities due to nuclear vibrations and rotations. The formalism uses the Superfluid Bardeen-Cooper-Schrieffer (BCS) [26] model below the critical excitation energy (option of EMPIRE specific level density) and Fermi gas model for above critical excitation energy. For the present calculations, the level density parameter ATILNO was scaled up by a factor of 1.06 for ^{55}Fe and scaled down by a factor 0.94 for ^{55}Mn in order to obtain the best fit with the present experimental data at all energies. Proton and neutron emission compete in the compound nucleus decay: increasing the emission probability of one particle affects the emission of all other particles. Therefore the level densities of both ^{55}Fe and ^{55}Mn play a role in the estimation of the proton emission cross section. In the absence of detailed measurements of all evaporation channels from compound system, our choice of ATILNO pa-

rameter deviation of 6% from the default value 1.0 to explain the proton emission cross sections as mentioned above, renders minimal changes from the known systematics for all channels. Results from EMPIRE-3.2.3 for excitation function with modified ATILNO values explain the present experimental data which agree with the available data library EAF-2010 [27], as shown in Fig.6.

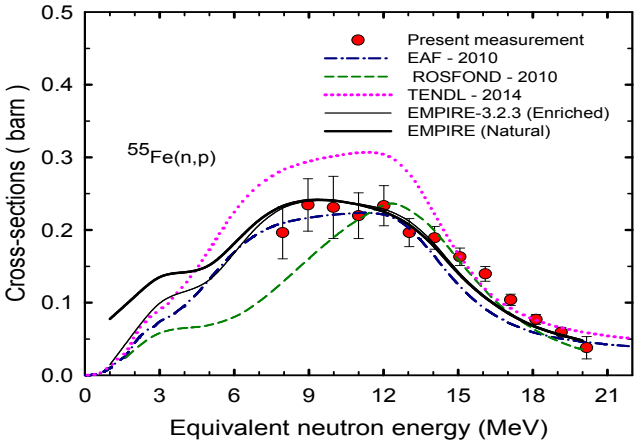

FIG. 6: The ^{55}Fe(n,p) cross-section as a function of equivalent neutron energy along with various evaluation results (in text) and EMPIRE - 3.2.3 calculations.

In the Fig.6, there are two curves (thin solid and thick solid) from EMPIRE-3.2.3. The thin solid curve is obtained considering the pure (100%) ^{55}Fe(n,p) reaction cross-section, whereas the thick solid curve corresponds to calculation with inclusion of contributions from other possible channels ^{53}Fe(n,p),^{56}Fe(n,p), ^{57}Fe(n,p) as the ^{nat}Cr [^{50}Cr(4.345%), ^{52}Cr(84.0%), ^{53}Cr(9.50%), ^{54}Cr(2.365%)] target is used in the present experiment. The theoretically calculated values of EMPIRE-3.2.3 code are in good agreement with our measured values. The present result on ^{55}Fe(n,p) cross-section by surrogate reaction method also follow closely the data files TENDL-2014 [28] and ROSFOND-2010 [29] between 13-20 MeV. In the neutron energy range of 7 MeV to 12 MeV measured cross-sections data are in reasonable agreement with EAF-2010 while TENDL-2014 , and ROSFOND-2010 show some discrepancy with the present measured data. As expected, this agreement with EAF-2010 is due to the normalization of the evaluation data to 14.5 MeV neutron induced reactions.

Generally, it is assumed that the production of hydrogen contribution due to ^{55}Fe(n,p) reaction is negligible in fusion reactor calculations. However, its inclusion can lead to increase in the hydrogen generation as the neutron induced proton emission cross sections at 14 MeV for various isotopes such as ^{54}Fe(n,p)$\sim$ 400 mb [30], ^{55}Fe(n,p)$\sim$ 200 mb (present work), and ^{56}Fe(n,p)$\sim$ 140 mb [30] are comparable. Therefore, the reactions ^{54,55,56}Fe(n,p) compete for hydrogen production.

In summary the ^{55}Fe(n,p) cross-sections have been measured in the equivalent neutron energy range of 7.9 MeV to 20.1 MeV by employing surrogate reaction method. The compound nuclei ^{56}Fe and ^{47}Ti are populated in ^{52}Cr(^{6}Li,d)^{56}Fe* (surrogate of ^{55}Fe(n,p)) and ^{45}Sc(^{6}Li,α)^{47}Ti* (surrogate of ^{46}Ti(n,p)) transfer reactions. The ^{55}Fe(n,p) cross-sections are then obtain in the excitation energy range of 19-30 MeV within the framework of surrogate ratio method. The known ^{46}Ti(n,p) cross-section values obtained from literature have been used as reference. The excitation energy is then converted to equivalent neutron energy by subtracting the neutron separation energy of the ^{56}Fe to obtain ^{55}Fe(n,p) cross-sections in the equivalent neutron energy range of 7.9 MeV to 20.1 MeV. The experimental results of ^{55}Fe(n,p) cross-sections have been compared with the available evaluation data libraries and EMPIRE-3.2.3 based calculations. By changing the level density parameter by 6% from the default value, the calculated and experimental cross sections are observed to be in good agreement. The present experimental data have also been compared with evaluated data libraries EAF-2010, TENDL-2014, ROSFOND-2010. The data of EAF-2010 library found to be reasonably consistent with the experimental data. The present measurement using surrogate reaction method will be useful to improve and update the different data libraries and opens up the possibility of measuring important compound nuclear reactions involving unstable targets with relevance to fusion technology.

The authors are thankful to R. Forrest, International Atomic Energy Agency (IAEA), for encouraging us to carry out the present measurement and M. Herman, Brookhaven National Laboratory (BNL) for his guidance and helpful discussion during the calculations with EMPIRE code. We are also grateful to S. M. Qaim, Julich Research Centre, Germany; R. Capote, IAEA, Austria; for their interest and valuable suggestions in this work. We are thankful to the Pelletron-LINAC staff for smooth operation of the accelerator during the experiment.

[1] ITER Physics Basis Editors, ITER Physics Expert Group Chairs and Co-Chairs, ITER Joint Central Team and Physics Integration Unit, ITER EDA., Nuclear Fusion, 39, 12, 2137-2174 (1999).

[2] U.S.Congress, Office of Technology Assessment, Starpower: The U.S. and the Internnational Quest for Fusion Energy, OTA-E-338 (Washington, DC: U.S. Government Printing Office, October 1987)

[3] H. Iida *et al.*, Nuclear Analysis Report (NAR) ITER, G73 DDD2 W0.2, July (2004).

[4] A. Wallner *et al.*, Journal of the Korean Physical Society 59 1378-1381 (2011).

[5] R.A. Forrest, Fus. Eng. Des. **81**, 2143-2156 (2006).
[6] R.C. Haight, 'Neutron Cross-section for fusion', Proceeding of international conference on nuclear cross-section for technology, held at University of Tennessee Knoxville, TN, October 22-26 (1979).
[7] R.A. Forrest, Fus. Eng. Des. **43**, 209-235 (1998).
[8] S. Fetter *et al.*, Fus. Eng. Des. **6**, 123-130 (1988).
[9] R.A Forrest *et al.*, UKAEA FUS 552, EURATOM/UKAEA Fusion, March, (2009).
[10] R.A. Forrest, Energy Procedia 7, 540-552 (2011).
[11] L.R.Greenwood and D.L.Bowers, Sixth ASTM-EURATOM Symposium on Reactor Dosimetry Jackson Hole, Wyoming, USA, June 1-5, (1987).
[12] J.D. Cramer and H.C. Britt, Phys. Rev. **C2**, 2350 (1970).
[13] H.C. Britt and J.D. Cramer, Phys. Rev. **C2**, 1758 (1970).
[14] B.K. Nayak *et al.*, Phys. Rev. **C78**, 061602 (2008).
[15] V.V. Desai *et al.*, Phys. Rev. **C87**, 034604 (2013).
[16] V.V. Desai *et al.*, Phys. Rev. **C88**, 014613 (2013).
[17] J.E. Escher *et al.*, Rev. Mod. Phys. **84**, 353-397 (2012).
[18] S. Chiba and O. Iwamoto Phys. Rev. **C81**, 044604 (2010).
[19] A. Gavron, Phys. Rev. **C21**, 230 (1980).
[20] International Reactor Dosimetry and Fusion File - IRDFF 1.05 https://www-nds.iaea.org/IRDFF/
[21] M. Herman *et al.*, Nucl. Data Sheets, **108**, 2655-2715 (2007).
[22] W. Hauser and H. Feshbach, Phys. Rev. **C87**, 366 (1952).
[23] B. Pandey *et al.*, Nucl. Sci. and Eng. **179**, 313-320 (2015).
[24] R. Capote *et al.*, Nucl. Data Sheets **110**, 3107 (2009).
[25] A.J. Koning and J.P. Delaroche, Nucl. Phys. **A713**, 231 (2003).
[26] J. Bardeen and L. Cooper, Phys. Rev., **108**, 1175 (1957).
[27] EAF-2010: European Activation File: http://www-nds.iaea
[28] TENDL-2012: TALYS Evaluated Nuclear Data Library: http://www.talys.eu/tendl
[29] ROSFOND-2010: Updated Russian Library of Evaluated Neutron Data: http://www-nds.iaea.org/exfor/endf.html.
[30] D.G. Gardner, Nucl. Phys. 29, 373 (1962).